

Structural and metamorphic evolution of the Nanga Parbat syntaxis, Pakistan Himalayas, on the Indus gorge transect: the importance of early events

J. WHEELER

Department of Earth Sciences, Liverpool University, Brownlow Street, Liverpool L69 3BX, UK

P. J. TRELOAR

School of Geological Sciences, Kingston University, Kingston upon Thames KT1 3EE, UK

AND

G. J. POTTS

Department of Earth Sciences, Liverpool University, Brownlow Street, Liverpool L69 3BX, UK

Field relationships are as important as radiometric age data for unravelling the history of polycyclic metamorphic regions. Field and petrographic data were used to investigate such a region, the Nanga Parbat syntaxis — a major N-trending transverse structure in the Pakistan Himalayas. Continental rocks of the Indian plate are exposed in the core of this structure due to uplift relative to the surrounding and structurally higher amphibolites of the overthrust Kohistan Island Arc. In the Indus gorge, the Indian plate gneisses are migmatitic, highly deformed and cut by Himalayan granite sheets. Field relationships show that the migmatization pre-dates the emplacement of a suite of basic intrusive sheets (now amphibolites) which are themselves unlikely to be Himalayan; these amphibolite sheets are cut by the Himalayan granite sheets. There is therefore no genetic link between the granites and the migmatization: the latter might be Precambrian. During the pre-Himalayan evolution, an eastern group of metapelitic migmatites underwent biotite dehydration melting at granulite facies conditions, leading to the development of assemblages with garnet, orthoclase and kyanite. Melt was not completely lost and back-reacted during cooling to give biotite–kyanite coronas around garnets. A western group of orthogneisses is characterized by foliated muscovite and biotite; orthoclase is never found with either garnet or aluminium silicate. In this second group, partial melting and small-scale segregation gave rise to the migmatitic appearance, but melt was not lost and back-reacted fully to regenerate the micas.

The migmatites and basic sheets were strongly deformed at amphibolite facies during Himalayan collision, producing LS tectonites, mylonitic in places. This strong fabric was then tightly folded on large scale. The NNE trending fold is slightly oblique to the earlier N–S stretching lineation: this has been reoriented on the steep limbs, but its plunge remains shallow. No new fabric is seen associated with this folding. On the western margin, steeply plunging lineations are associated with shear bands in gneisses, indicating relative uplift of the syntaxis. In contrast, on the steep eastern margin, relative uplift of the syntaxis appears to have been due to rotation without the development of new fabrics. There is no evidence for further melting during this Himalayan evolution, so the granite sheets cannot have been derived locally. This study highlights the importance of distinguishing pre-Himalayan and Himalayan events in this polymetamorphic region, and the usefulness of field relationships in addition to geochronological constraints in such a task.

KEY WORDS Himalayas; geochronology; polymetamorphism; migmatites

1. INTRODUCTION

The timing of metamorphic events is critical information in constraining controls of metamorphism. An important aspect of orogenic evolution is the involvement of crust which had already been deformed and metamorphosed in previous events, together with cover sequences and other rocks which had no such prior

history. Distinguishing metamorphism related to the most recent orogenic event from that related to older events is therefore essential for orogenic studies. In the external parts of orogenic belts, this may be straightforward — for instance, in the Mont Blanc massif of the Western Alps, deformed yet otherwise little metamorphosed sediments lie unconformably on migmatites. Because the (Mesozoic) sediment deposition pre-dates the Alpine collision, the older migmatites relate to an earlier orogenic event. In the internal zones of orogens, the story may be less clear. Where basement and cover can be distinguished on lithological grounds, their metamorphic grade may be comparable and this could give the illusion that metamorphism was synchronous, even if that in the basement relates to a much older event. If units of metamorphic rock cannot be identified as basement or cover, the age of metamorphism becomes more problematic. Geochronology is a useful tool in unravelling metamorphic timing, but can be misleading if units of already metamorphic basement are reheated during orogenesis. Then, cooling ages can be reset, even if the minerals themselves crystallized long before.

In this paper we show how field relationships are critical to establishing relative timing of events, with reference to the Nanga Parbat basement massif in the Pakistan Himalayas. This region consists of complexly deformed migmatites and amphibolites which are cut by a suite of leucogranites of Himalayan age. The age of the metamorphism is currently of interest, with respect to its possible link to the leucogranite suite, and to the recent reporting of very young U/Pb ages from some migmatites (Zeitler *et al.* 1993). The structural history of the interior of the massif is also important as it appears to be the locus of rapid recent uplift (Zeitler 1985; Butler and Prior 1988b), accommodated at least in part by thrusting at the margins: the ages of fabrics within the massif are relevant for understanding this. We therefore report both the structural and metamorphic aspects of the massif along a detailed transect.

2. REGIONAL SETTING OF THE NANGA PARBAT MASSIF

Two major collision events characterize the evolution of the NW Himalayas as seen in northern Pakistan. In the first event, between 100 and 85 Ma, the Kohistan–Ladakh terrane, interpreted as an island arc, was sutured to the Asian continental plate (Coward *et al.* 1986; Treloar *et al.* 1989a). In the second collision Indian continental crust was thrust beneath the Kohistan Island Arc, giving rise to intense deformation within the Indian plate gneisses and cover sediments (Treloar *et al.* 1989a). The present contact between these two structural units is the Main Mantle Thrust (MMT). Later in the collision event, the MMT was raised around a crustal-scale N–S trending structure, the Nanga Parbat syntaxis (Wadia 1931; 1932), which has the effect of exposing Indian plate gneisses of the MMT footwall well into the internal parts of the Himalayan orogen (Figure 1). Its northern boundary comes close to, but does not intersect, the Northern Suture (Butler *et al.* 1992): arc rocks to the east, distinguished as the Ladakh Island Arc, are thus continuous with those to the west. Rocks from above and below the MMT have different metamorphic histories. In the Kohistan arc, amphibolite and granulite facies metamorphism pre-dates the second collision event. In the Indian plate gneisses, amphibolite and granulite facies rocks (Treloar *et al.* 1989a; Pognante *et al.* 1993), cordierite migmatites (Zeitler *et al.* 1993), and eclogites (Tonarini *et al.* 1993) are found. This diversity is reflected in radiometric dates: cordierite migmatites may be as young as 3 Ma, the eclogites crystallized at ca. 50 Ma and, in the Indus gorge, gneisses show Precambrian ages for zircon cores.

Some, but not all, transects through the syntaxis show it to have an antiformal structure. The syntaxis is of significance not only as a window into the footwall gneisses which must have been deeply buried beneath the Kohistan island arc, but also as an indicator of deep-seated processes which have drastically modified earlier collisional geometries and are still continuing (Zeitler 1985; Butler and Prior 1988b). To unravel the history of the syntaxis, it is essential to distinguish early events which may have affected the Indian plate long before collision, from those which link to these recent events: the Palaeozoic and Proterozoic ages of some gneisses in the Indus gorge (Chamberlain *et al.* 1989) allow the possibility that earlier, Precambrian, fabrics may be present within the syntaxis, and may even be dominant. Coward (1985) and Coward *et al.* (1986) proposed that the present structure is an antiform formed by buckling of the MMT, whereas Madin *et al.* (1989) suggested it to be uplifted along a crustal-scale dextral reverse fault along its western margin. The trend of

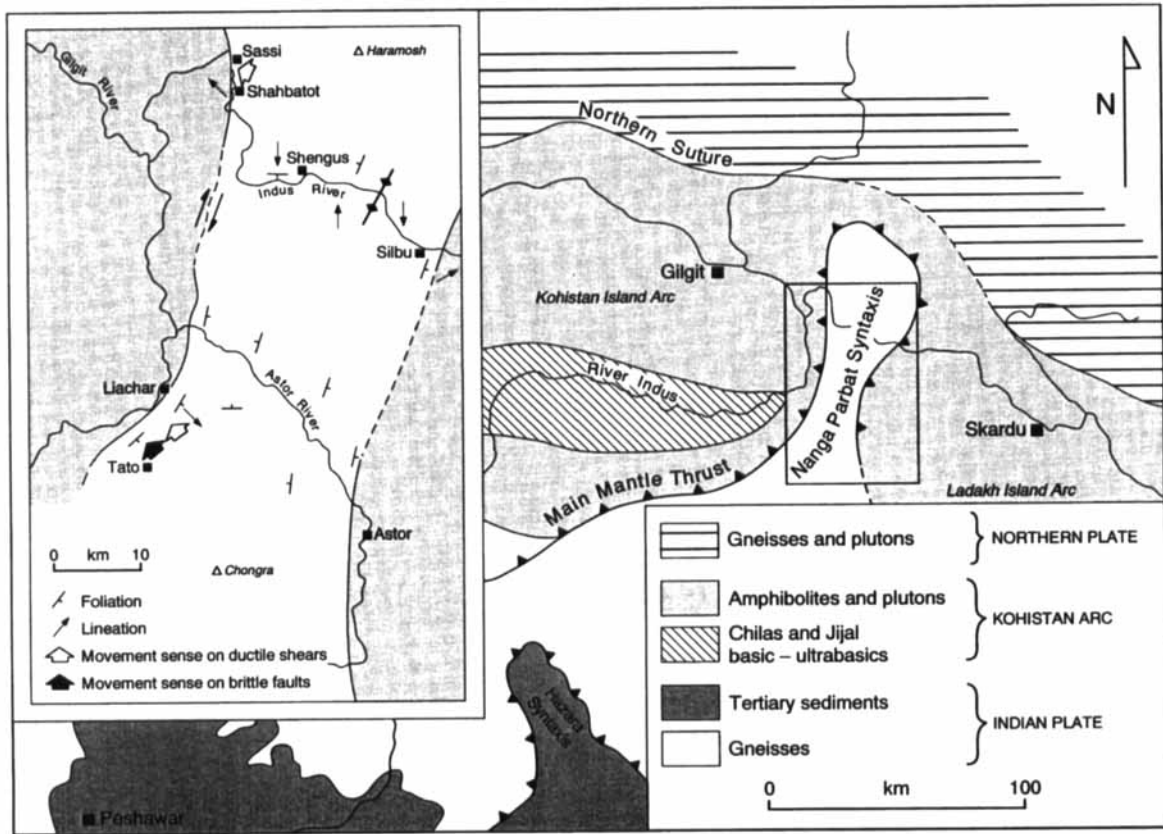


Figure 1. Main tectonic elements of the Pakistan Himalayas and (inset) location map for Indus Gorge traverse of the Nanga Parbat syntaxis, showing movement senses within the syntaxis fabrics where known. Foliations in the Astor River region from Misch (1949)

the syntaxis suggests a component of shortening at a high angle to the convergence between the Asian and Indian plates. This has been linked with a postulated pinning at the NW tip of the main Himalayan thrust belt of India, which would give a SW-directed component of movement in the Nanga Parbat region (Coward *et al.* 1986). Detailed investigation has shown that the western margin of the syntaxis is much more complex than a simple buckle-fold model would suggest: in the north at Sassi (Figure 1) several generations of steep faults parallel the margin of the syntaxis and are dextral strike-slip (Butler *et al.* 1989). Late faulting is important further south, at Liachar, where the Indian plate gneisses have been thrust over Indus valley river gravels with a NW movement sense (Butler and Prior, 1988b); a great thickness of gneisses (with fabrics parallel to the thrust faults) is seen in the hanging wall. These augen gneisses show a well-developed SE plunging stretching lineation with abundant top to NW shear sense indicators, and represent fabrics developed at deep levels in the shear zone (the Tato shear zone), of which the Liachar thrust is a part (Butler and Prior 1988a).

The aim of this paper is to discuss the evolution of the interior of the syntaxis with reference to new observations on a transect along the Indus gorge. Building on a preliminary model (Treloar *et al.* 1991), we have constructed a structural sequence on the basis of observed overprinting relationships and integrated this with new metamorphic information. Late, brittle features will not be discussed here, although they are common throughout the syntaxis and are important on the western margin (Butler *et al.* 1989). In the following sections we describe firstly the structure along the transect and secondly the metamorphic history. Finally, we synthesize these data to present an internally consistent model for the evolution of the syntaxis along this transect and discuss the wider implications of our results.

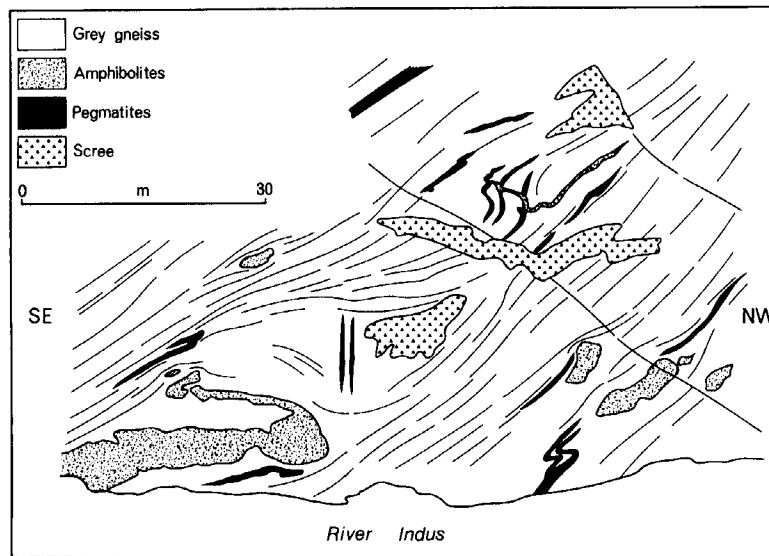


Figure 2. View from road between Shengus and Silbu (Figure 1), looking SW to opposite side of Indus gorge, of folded amphibolite sheets and pegmatites. See text for details. Drawn from field sketch and photographs (see Figure 6b)

3. STRUCTURE OF THE NANGA PARBAT SYNTAXIS ALONG THE INDUS RIVER GORGE

3a. Structural sequence as deduced from field relationships

Most of the syntaxis consists of grey and brown gneisses, sometimes garnetiferous, sometimes migmatitic. Some grey augen gneisses resemble deformed plutonic rocks of granitic or granodioritic composition, though they contain, in places, calc-silicate pods of sedimentary origin. Brownish migmatitic gneisses are likely to be metasediments, as are distinctive pinkish gneisses with lilac garnets associated with calc-silicate pods and, less commonly, diopside marbles. No structural criterion allows the relative ages of these gneisses to be determined. At least one major deformation event has led to gneissic banding in all these rocks, associated with syntectonic granite and centimetre to metre-scale pegmatite veins. As well as being strongly banded, the gneisses usually show planar and linear fabrics defined by the shapes of individual biotites and by the shapes of aggregates of other minerals. A distinctive suite of amphibolite sheets appears within the gneisses. These are interpreted as deformed basic dykes and/or sills. They have a fine-grained, homogeneous fabric. Although the sheets are strongly foliated in many places, minor discordances with the banding in the wall rocks are common.

The amphibolite sheets are not seen to cross-cut each other and we assign them a single age. In places the sheets cross-cut pre-existing banding that includes distinct pegmatitic segregations (Figure 2 top right; Figure 3; see also figure 3a of Butler *et al.* 1992), so there must have been a pre-sheet phase of deformation that produced a gneissic banding. As there is also manifestly post-intrusion deformation, the amphibolite sheets represent a crucial time marker in the history of the basement gneisses, analogous to the Scourie dyke swarm within the Lewisian Complex (Sutton and Watson 1951). It is important to determine the relative contributions of both deformations to the observed fabrics. We now describe field evidence that demonstrates that the *gneissic banding* pre-dates the sheets, whereas the dominant *planar and linear shape fabrics* post-date the sheets.

The amphibolite sheets are commonly subparallel to banding and planar shape fabrics in the gneisses, but, in these instances, the sheets carry strong internal fabrics and therefore the present geometry could be transposed. In a few key locations, high angle contacts are preserved (Figure 2 top right; Figure 3). These show that the sheets post-dated the migmatitic banding. As discussed in the section on metamorphism, this banding is interpreted as due to partial melting rather than subsolidus processes. Nowhere is there any

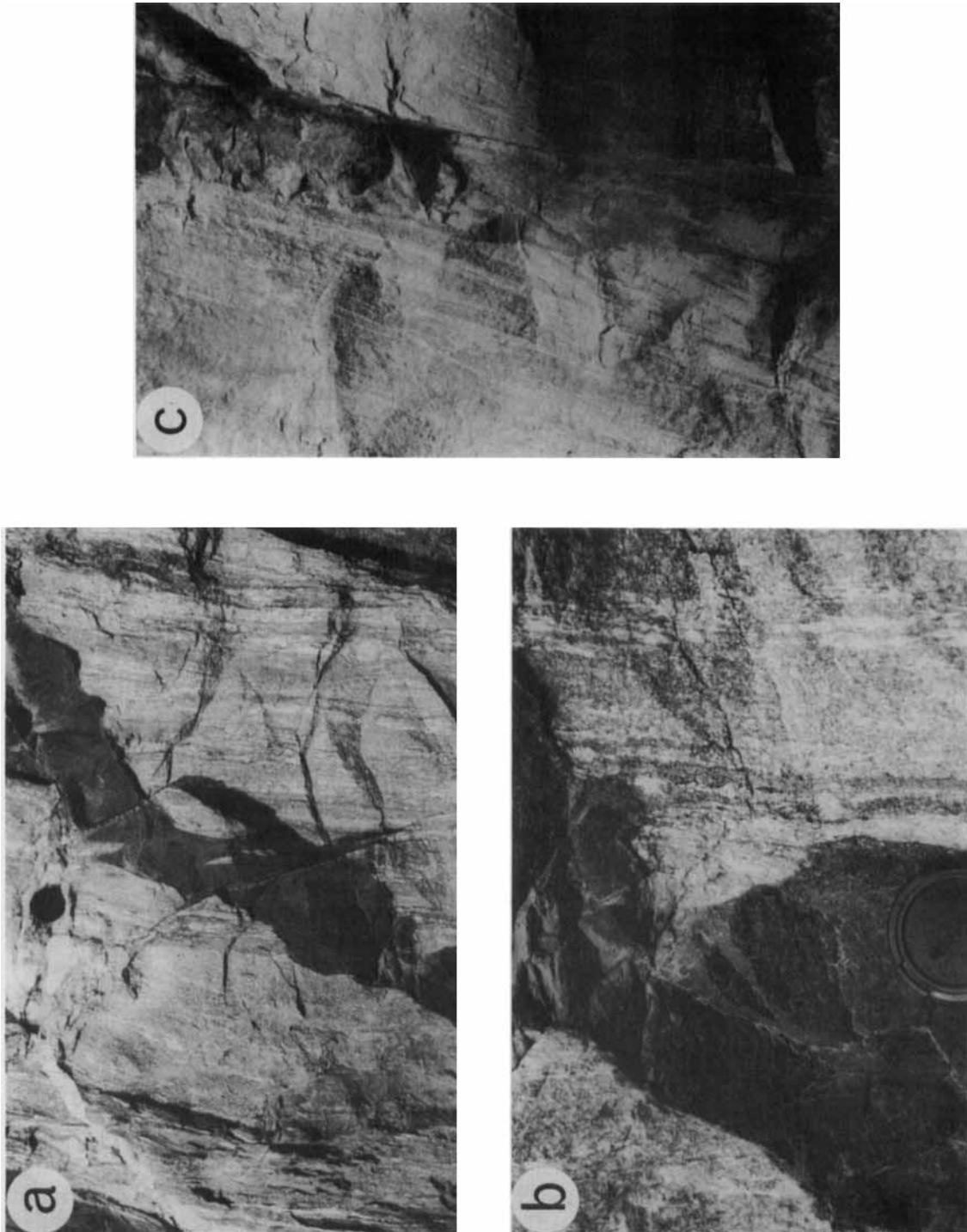


Figure 3. (a) Strongly discordant amphibolite sheet cutting migmatitic banding. (b) Closer view of lower part of (a). (c) Low angle discordance between amphibolite sheet and gneissic banding

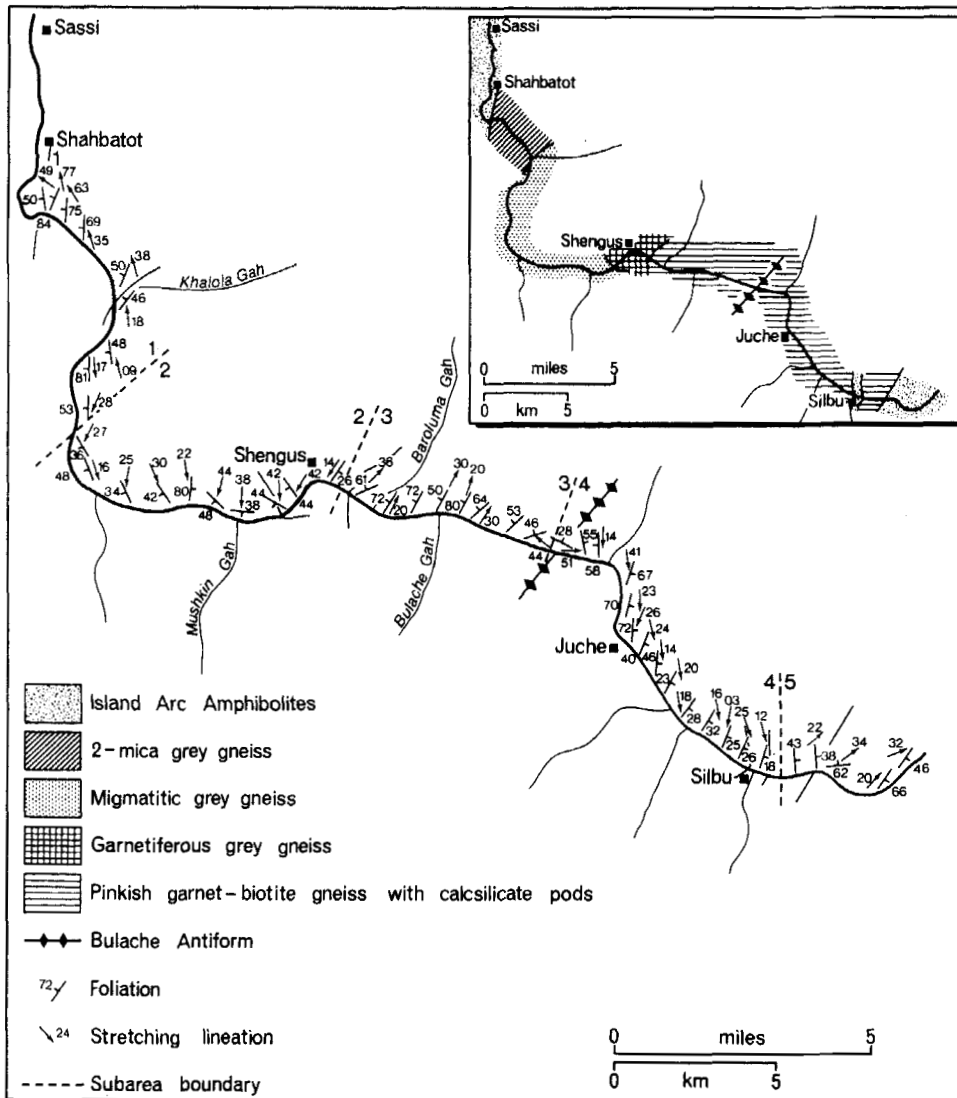


Figure 4. Lithology, principal foliations and stretching lineations, and structural subareas along the Indus Gorge traverse. Subareas are numbered at their borders. The pinkish gneisses correspond roughly to the Shengus gneiss of Chamberlain *et al.* (1989) and the three grey gneiss types to the Iskere gneiss of those workers

evidence that the sheets were themselves migmatized, or injected by leucosomic material from surrounding wall rocks. We conclude that, as far as field criteria are concerned, the migmatization — which is responsible for the banding in the gneisses — entirely pre-dated the basic sheets.

Figure 2 shows that the sheets were both folded and boudinaged during subsequent deformation, indicating that they were less ductile than the wall rocks. However, wherever lineations within the amphibolites have been measured, they have been parallel to the general stretching lineation in the gneisses for that part of the transect. Contacts of amphibolites with gneisses have consistently contained that same direction. These general patterns show that in most of the traverse the observed sheets are highly strained and almost transposed with pre-existing structures. The dominant foliation and lineation clearly post-date the intrusion of the basic sheets. Local augen, in which sheets were folded, but partly protected adjacent gneisses from the intense deformation, occur sporadically. These augen preserve the early discordances, which show that the migmatitic banding in the gneisses pre-dates the sheets.

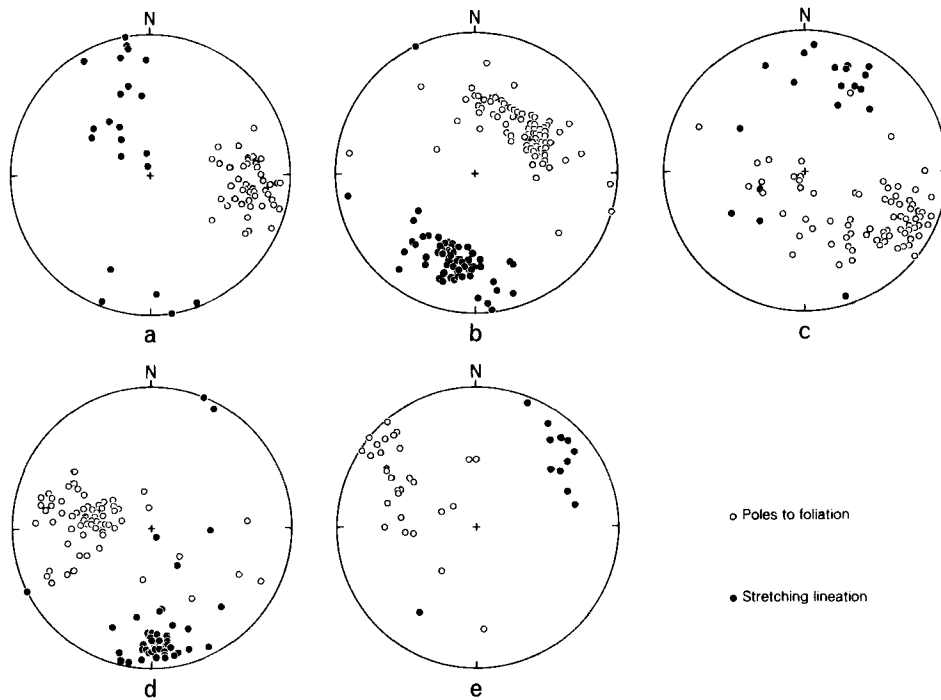


Figure 5. Equal-area lower hemisphere stereonet of foliation and lineation for the five subareas defined along the Indus Gorge traverse (see Figure 4). (a) to (e) are subareas 1 to 5

A suite of garnet granites and tourmaline pegmatites (distinct from the earlier migmatite-related pegmatites, which are cut by the amphibolite sheets) cross-cuts all these features, showing only local fabrics. This summarizes the structural and intrusion sequence within the Indian plate gneisses.

To the west of the syntaxis are amphibolites of the Kohistan arc, and to the east are similar Ladakh amphibolites. The latter are characterized by regular layering of amphibolites and foliated garnet granites; an identical association occurs in certain slivers *within* the Indian plate gneiss near the eastern limit of the syntaxis. A correlation of deformation history on structural criteria between these rocks, interpreted from regional data as part of an island arc sequence, and the Indian plate gneisses is not possible. Nevertheless, the slivers of Ladakh-type amphibolites within the gneisses of the syntaxis are effectively transposed parallel to the main foliation, implying that the main foliation is younger than the Ladakh island arc in this vicinity.

3b. Large-scale geometry

Figure 4 shows the structure and lithology along the traverse. From the great variety of gneiss types, we have distinguished four lithologies — all contacts are transitional, however. The gneissic banding defines an overall antiform in which much of the foliation is steeply dipping. Although almost all the gneisses are highly strained, some belts are intensely banded and mylonitic. Corresponding rock types do not appear on either side of the main antiformal closure (the Bulache antiform of Madin *et al.* 1989); the east side has slivers of Ladakh amphibolites and an abundance of pink gneisses and basic sheets, whereas the west side has more grey augen gneiss and fewer sheets. Chamberlain *et al.* (1989) and Madin *et al.* (1989) also distinguish separate groups of gneiss on either side of the syntaxis: the grey augen gneisses on the west of the syntaxis correspond roughly to their 'Iskere orthogneiss' and the pink gneisses correspond to their 'Shengus paragneiss'.

In contrast with the relatively simple arch of foliation, the lineations show complex swings (Figure 4). From west to east we identify six structural subareas defined on the basis of lineation and foliation orientations (Figure 5). The westernmost part of the traverse is not discussed in detail here; it contains gently



Figure 6. (a) Photograph of steep eastern contact of syntaxis with Ladakh amphibolites (dark rocks on right of picture) against Indian plate gneisses (pale rocks on left). View from road looking east and up. The col through which the contact passes is about 1500 m above the road. (b) Photograph of amphibolite sheets shown in Figure 2

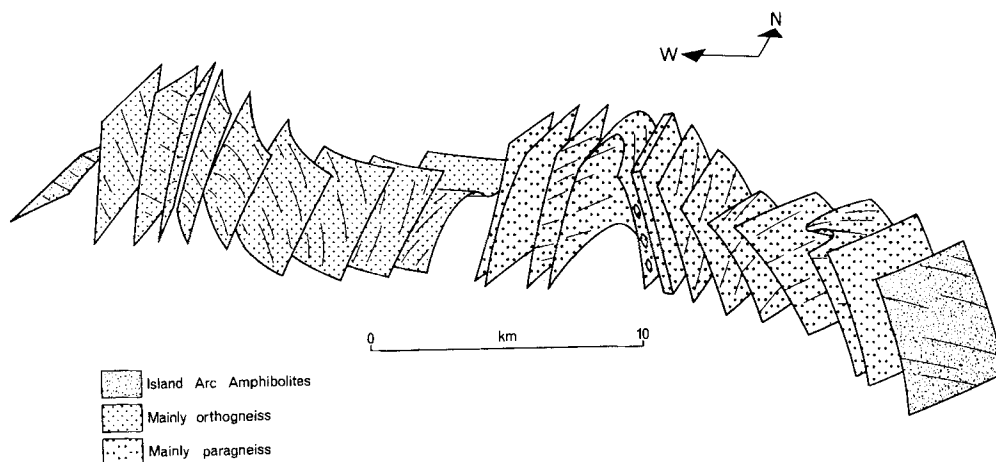


Figure 7. Synoptic view from SE of foliation form surfaces and lineations (shown schematically on foliation surfaces) in Indus Gorge traverse

NW plunging lineations within Kohistan amphibolites. Butler and Prior (1988a) confirm lineations related to SSE directed overthrusting of the Kohistan terrane in this area.

Subarea 1 has vertical or steep NW plunging lineations in a steep belt of augen gneisses within the syntaxis. This belt has common shear bands which dip steeply W and show a down to the W movement sense. This is the only zone in the syntaxis which exhibits obvious E-side up shear sense indicators, and we will refer to it as the Sassi steep belt. In the south of this subarea lineations become shallow to adopt the trend characterizing subarea 2.

Subarea 2 contains gently S-plunging lineations within often migmatitic grey and brown gneisses.

Subarea 3 has gently N plunging lineations within garnetiferous mica schists and scattered occurrences of other lithologies. The foliation dips steeply NW.

Subarea 4 lies on the other (east) side of the main Bulache antiformal axis which trends NNE. As much of the syntaxis shows N–S trending lineations, these are arched over the fold to plunge N on the west side and S on the east side in Subarea 4. Occasional shear bands show top to the S movement.

Subarea 5 is close to the eastern contact, where lineations swing to plunge gently NE. Lineations of this trend continue eastwards within the Ladakh amphibolites. These lineations are parallel to the regional lineations recorded in the Ladakh Himalayas (Brunel 1985). At the eastern contact (Figure 6a) the MMT is subvertical or overturned and shows minor open folds, but is unmodified compared with the west end of the transect, where it is dissected by late shears and faults.

The structure of the transect is summarized in Figure 7. The general trends of foliation and lineation summarized in the subareas omit local complexities. In a few outcrops of grey augen gneisses both pure L, LS and pure S fabrics are found, and locally L varies in plunge from vertical to horizontal. L may not bend progressively between these orientations, but instead L tectonites of different orientations are separated by pure S tectonites. These resulted from locally complex strains around low strain lozenges of augen gneiss. Regions with obvious fold overprinting relations are also rare. We interpret the lineations as stretching, as indicated by the elongation of felsic clots in the various gneisses. There is no direct information available on the amplitude of the antiformal structure, but it might have extended to at least 10 km above road level as suggested in Figure 8 (there are no grounds for attempting a detailed construction of the fold shape — for example, using the Busk construction). The lithological differences between the east and west of the antiform have been interpreted by us as resulting from thrust slices within the syntaxis which were then folded (Treloar *et al.* 1991). There are particularly high strain rocks in places within the transitional contact zone; these might indicate a major shear zone, but could also be due to local strains at the contact between rocks types of contrasting rheologies. The distinction, made in that work, between a ‘sillimanite-bearing’ and a

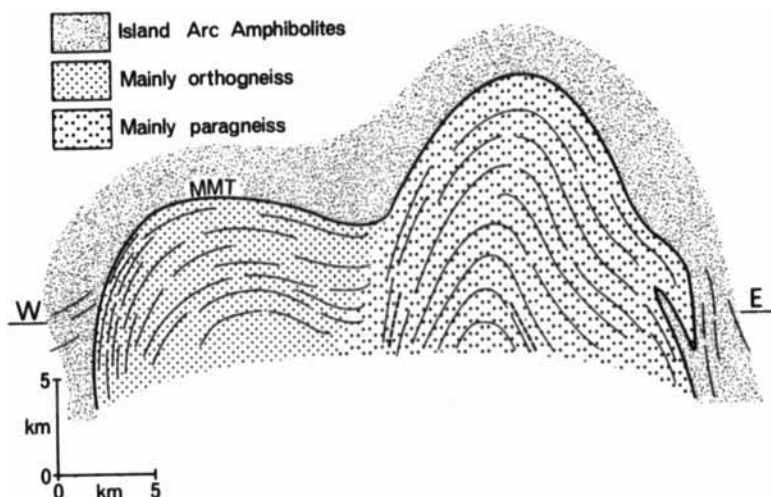


Figure 8. Speculative cross-section showing possible form for the antiformal structure of the Indus Gorge traverse

'kyanite-bearing' nappe within the Shengus gneiss has been shown to be illusory from additional petrographic observations (see later); commonly both aluminium silicate polymorphs occur together.

3c. Age of the structural sequence

We use regional criteria here to suggest the age of the sequence, because existing cooling ages do not give the age of deformation directly. U/Pb crystallisation ages of zircons (Chamberlain *et al.* 1989; Zeitler *et al.* 1989) of 1850 Ma for the Iskere gneiss and, in contrast, 400–500 Ma for the Shengus gneiss (from a metagranitoid within this dominantly metapelitic unit) also do not date any particular deformation, but highlight the lengthy pre-Himalayan history of the gneisses. In the Kohistan and Ladakh amphibolites, which are known to be Mesozoic (Pudsey 1986), the lineations must be broadly Himalayan in age, although sometimes pre-dating the main India–Asia collision (e.g. deformation in the Kamila shear zone is pre-80 Ma; Treloar *et al.* 1989b). In the Indian plate gneisses, indirect arguments must be used to suggest an age for the main (post-basic sheet age) fabrics. In the Hazara area, there was extensive Himalayan age deformation in Indian plate gneisses and metasediments in the footwall to the MMT (Treloar *et al.* 1989a) during emplacement of the Kohistan island arc. Lineations here trend N–S. Butler *et al.* (1989) record SSE directed ductile overthrusting during this emplacement event in the area immediately west of the Nanga Parbat syntaxis and south-directed overthrusting persists as far south as the Salt Ranges. Although detailed studies elsewhere in the MMT footwall show spatial and temporal variations of shear direction, these generally all have a southward movement component. For instance, during the development of the Hazara syntaxis, Bossart *et al.* (1988) record an evolution from SW to SSE directed thrusting. In general, Indian plate gneisses from beneath the MMT south and west of the Nanga Parbat syntaxis display a thick zone of Himalayan age deformation and show broadly consistent N–S lineations related to southwards emplacement of the Kohistan island arc (Brunel 1985; Coward *et al.* 1986). If the main fabric in the Indian plate gneisses in the Nanga Parbat syntaxis were Himalayan, it would fit within this scheme. Finally, the transposition of Ladakh amphibolite slivers within the Indian plate gneisses near the eastern syntaxis margin is strong evidence that the main fabric in the gneisses there is Himalayan. For these reasons we conclude that the main fabric throughout the gneisses of the Indus gorge transect, which has a dominantly N–S lineation, is of Himalayan age, was formed during overthrusting of the Kohistan island arc and was subsequently folded during syntaxis growth.

The age of the basic sheets is unlikely to be post-collision. Basic magmas are difficult to generate and emplace in tectonic settings involving crustal thickening and compression, and no post-collisional basic

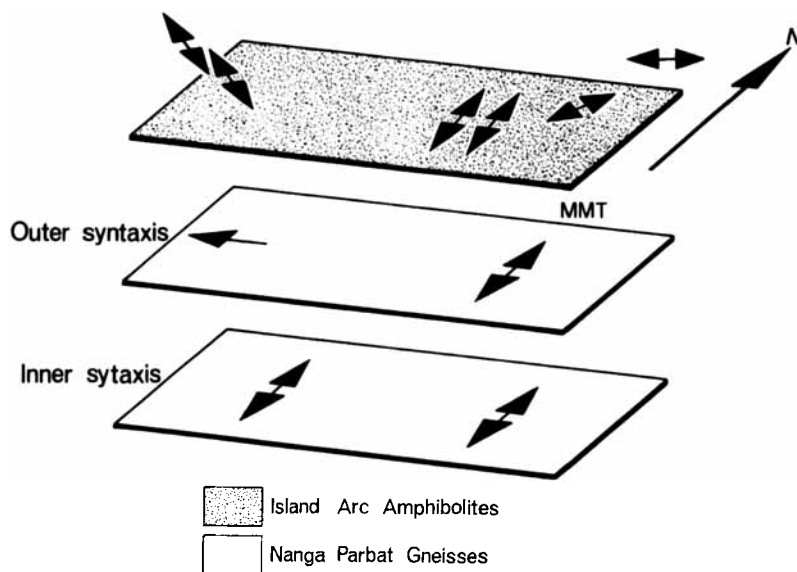


Figure 9. Configuration of lineations resulting from unfolding the observed pattern of foliation and lineation on the assumption that the antiform resulted from buckling. Double-headed arrows indicate unknown shear sense; single-headed arrow shows motion of top where known

migmatism is known from other nearby parts of the Indian plate. The latest episode of basic magmatism which affected the Indian plate in N Pakistan and NW India was that which produced the Permian Panjal traps (Vannay and Spring 1993). The basic sheets in the syntaxis may be of this age. Alternatively, they could be still earlier — Proterozoic dyke swarms are well known in Precambrian cratonic regions and the Proterozoic zircon ages from the gneisses highlight this possibility. In either instance, the migmatization predates the basic sheets and is therefore not related to the Tertiary Himalayan collision: it could be Palaeozoic or even Precambrian.

3d. Interpretation of Himalayan structural history

Figure 8 suggests that the syntaxis could have been produced by buckling the subplanar MMT and rocks beneath which were foliated roughly parallel to it. The tightness of the major antiform implies that some flattening would have occurred across the syntaxis in addition to the buckling, but new vertical fabrics in the core of the syntaxis are not seen. The main corollary of this model is that the antiform can be unfolded to gain an idea of the original relative dispositions of the lineations above and below the MMT. Figure 9 shows that this implies a strong variation in lineation trend. In particular the lineations in the Sassi steep belt (Figure 1; west side of Figure 8) become E–W or NW–SE oriented, with an associated top to W or NW movement sense. At a corresponding level (just below the MMT) on the east side, lineations are N–S. Above the MMT, within the amphibolitic thrust sheets, lineations are NW–SE in Kohistan and NE–SW in Ladakh.

This complex picture is difficult to reconcile with the dominantly S-directed overthrusting expected during collision. It is likely that the Kohistan and Ladakh parts of the island arc did follow the convergent movement trends implied by the lineation pattern (Brunel 1985), so the locally NW-directed shear predicted to have developed beneath the MMT would be highly anomalous. Thus although the buckle-fold model does explain the overall foliation pattern of the syntaxis, it does not completely explain the lineation pattern. In their present orientation, fabrics in the Sassi steep belt are consistent with uplift of the syntaxis relative to the Kohistan amphibolites and it is probable that they represent a late shear zone aiding relative uplift of the Indian plate gneisses. The Sassi steep belt is now west-dipping with an apparently near-vertical, slightly extensional, movement. Possibly the structure has been backsteepened after formation as an original E-dipping reverse

structure; alternatively, moderate shear strain on an E-dipping zone would still give W-dipping fabrics. In either instance, the shear zone would be analogous to, although much steeper than, the SE dipping overthrust fabrics of the Tato shear zone to the south (Butler and Prior 1988a). Both the Sassi and the Tato shear zones allow uplift of the syntaxis. In contrast, to the west, we find no evidence on the east margin for shearing, other than that associated with broadly S directed movement which has since been rotated.

4. METAMORPHIC HISTORY

In this section we describe the metamorphic development of the Indus gorge rocks and relate this to the structural history by tying microstructures to the fabrics which were observed in the field and described earlier. There is a great variety of gneiss types within the gorge, but we find systematic petrographic differences between the grey augen gneisses of 'Iskere' type (Chamberlain *et al.* 1989), dominant in the west, and the pink 'Shengus' gneisses in the east. All the gneisses contain quartz and (with rare exceptions) plagioclase — more abundant in the Iskere type. Differences are more apparent in the AKFM minerals present, as summarized in Table 1, which includes rocks from throughout the gorge section. The lists of AKFM minerals are not intended to imply equilibrium assemblages: the rocks commonly show textural and mineralogical evidence for disequilibrium, the occurrence of both kyanite and sillimanite within the same thin section being the most obvious example. Figure 10 gives further examples of textures which can be interpreted in terms of disequilibrium between AKFM phases. It should also be noted that muscovite, if present at all, is a minor phase in the Shengus gneisses, where the main AKFM phases are some combination of ky, sil, grt and bt. We will interpret petrographic data with the aid of petrogenetic grids and geothermobarometry based on probe data, although the latter has been of limited use because of retrograde re-equilibration.

4a. *Shengus gneiss: textures*

Figure 10 shows key textures in the Shengus gneiss. Sillimanite is sometimes preserved as needles, crudely aligned in places, within garnets (Figure 10a). Commonly, garnet is surrounded by aggregates of decussate biotite and kyanite (Figure 10b); further from the margins of the garnets these aggregates become fine-grained foliated bands of the two minerals (Figure 10c and 10e). Garnet and perthitic orthoclase commonly appear as porphyroclasts with ragged margins in a foliated matrix; usually modal banding parallels the sometimes weak shape fabric (Figure 10c). Orthoclase shows core and mantle structure with small new grains round the edges forming trails into the matrix, and in places bands of subgrains within the old grains (Figure 10d). Quartz showing undulose extinction may form ribbons or more equant grains. Muscovite is not present in large amounts, and is generally found as randomly oriented grains cross-cutting biotite fabrics (Figure 10f). This summary disguises the great variety of textures seen — two important variants are the occurrence of biotite–kyanite rims around garnet when no other potassic phase is seen in the rock, and the occurrence of fibrolite mats in the foliated matrix outside garnet grains (Figure 10f).

4b. *Shengus gneiss: interpretation*

It is clear from the orthoclase — aluminium silicate association that the rocks have experienced high temperatures. The dominance of AKFM phases and quartz shows that the rocks are metapelites and, at some stage, must have contained hydrous phases such as muscovite, which has broken down either by dehydration or as part of a melting reaction (Le Breton and Thompson 1988; Vielzeuf and Holloway 1988). In addition, the kyanite–biotite association rimming garnet is interpreted as the product of a reaction between garnet and other phases, at least one of which must have been potassic. This gives the following provisional sequence of events.

1. Sillimanite needles foliated in early deformation; orthoclase may have been present.
2. Garnet overgrows sillimanite fabric; orthoclase may have grown at this stage.

Table 1. Mineralogy of dominant gneiss types in the Indus gorge, excluding the amphibolite sheets. Only AKFM minerals are mentioned. Mineral abbreviations after Kretz (1983). The number of thin sections with each assemblage is a rough guide to their importance

Assemblage		Number recorded			
Equally common in Shengus and Iskere Gneisses					
	Grt	Bt		16	
Ky/Sil	Grt	Bt	Ms	15	
Ky/Sil	Grt	Bt		5	
		Bt		4	
		Bt	Ms	4	
	Grt	Bt	Ms	4	
Ky/Sil		Bt	Ms	3	
Present in Shengus, never in Iskere Gneisses					
Ky/Sil	Or	Grt	Bt	6	
Ky/Sil	Or	Grt	Bt	5	
Present in Iskere, rare in Shengus Gneisses					
	Or		Bt	Ms	5
	Or		Bt		3
	Or			Ms	2
Total				72	

3. Garnet partially reacts with other phase(s) to biotite+kyanite.
4. Biotite and kyanite rims were streaked out during subsequent intense deformation, forming bands which wrap garnet. Growth and deformation of the biotite–kyanite rims could have been synchronous, but alternatively the two events were separated by a long time period. Orthoclase partly recrystallized during the same deformation, giving rise to core and mantle structure, and bands of recrystallized orthoclase in the foliation.
5. Sporadic development of post-tectonic muscovite and sillimanite.

Figure 11 shows relevant reaction lines in a pelitic system for a specific bulk-rock Fe/Mg ratio of 1 (Vielzeuf and Holloway 1988). Divariant reactions are shown as univariant lines on this grid, so it cannot be used in a completely rigorous way. The reaction lines involving ferromagnesian phases vary considerably as a function of the Fe/Mg ratio of the system; for instance biotite+aluminium silicate reacts to garnet+muscovite with increasing pressure, but at much lower pressures for more iron-rich compositions (Le Breton and Thompson 1988). The common occurrence of the equilibrium assemblage garnet–muscovite–sillimanite in some pelites shows that this reaction line, and the invariant point A, must lie within the sillimanite stability field for some pelitic compositions. However, in the gneisses we describe, biotite+kyanite are interpreted as being in equilibrium as they grew simultaneously. So the rocks have an Fe/Mg ratio allowing biotite+kyanite to have a stability field, and the invariant point A is likely to be in the kyanite stability field. Thus we consider the grid to be broadly applicable to the rocks investigated here. The various muscovite breakdown reactions are insensitive to the Fe/Mg ratio because, although the phengite component has an effect, it stabilizes muscovite to only ca. 10°C higher than pure phengite-free muscovite.

After stage 2, the rocks contained orthoclase and garnet, among other phases. We assume that the rocks were originally pelites and at some stage contained free water; in this instance orthoclase cannot have been stable on the prograde path, as sillimanite appears to have been stable at an early stage. It is then difficult to envisage the orthoclase–garnet association developing other than by fluid-absent partial melting. Firstly, note that the absence of cordierite and the association garnet–sillimanite implies pressures above 6 kbar (Figure 11). At lower pressures, muscovite can dehydrate on a prograde path to give orthoclase and sillimanite. However, at pressures above those of invariant point B, muscovite melts in the presence of water leaving only aluminium silicate; orthoclase does not form. In contrast, consider a fluid-absent situation. This

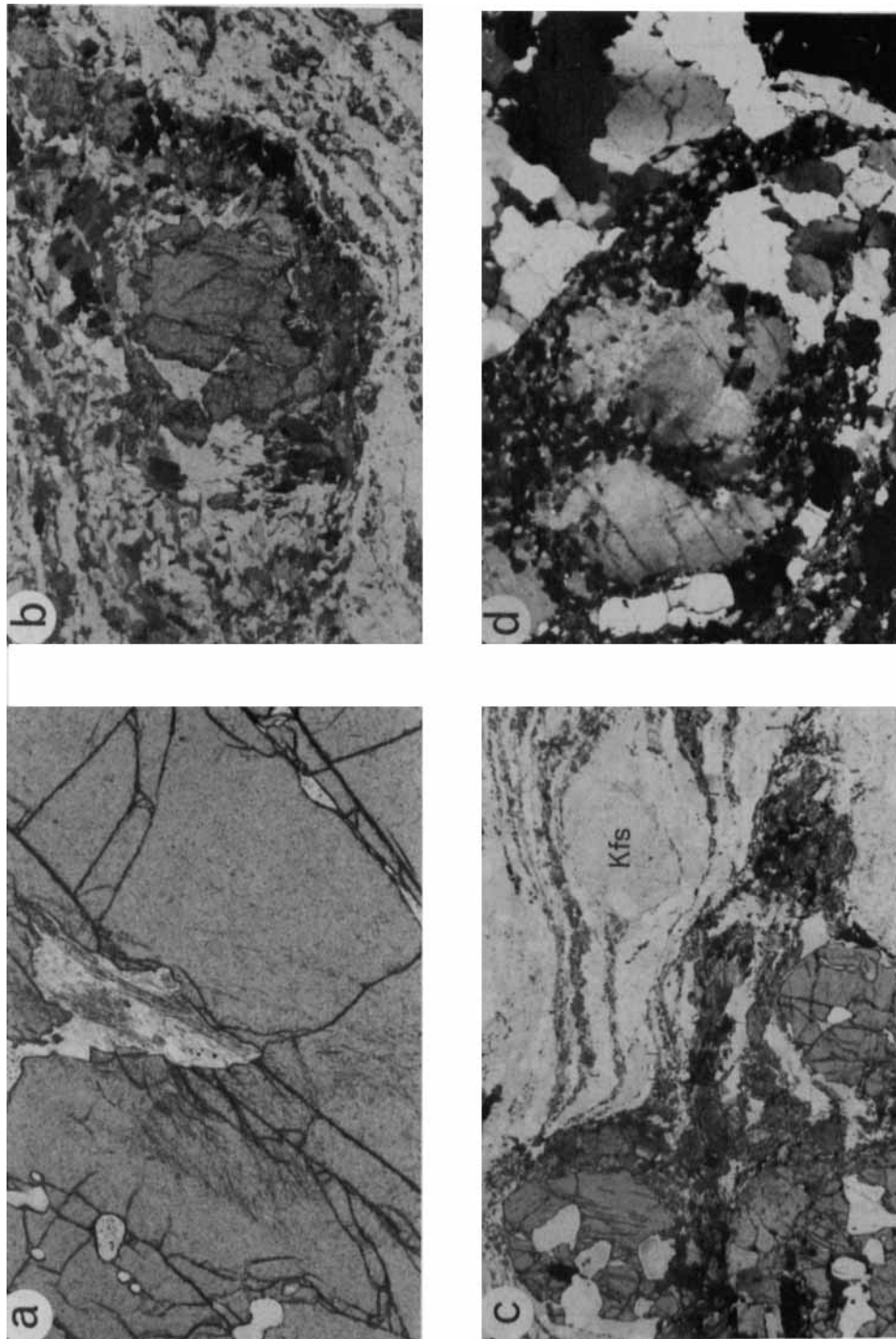
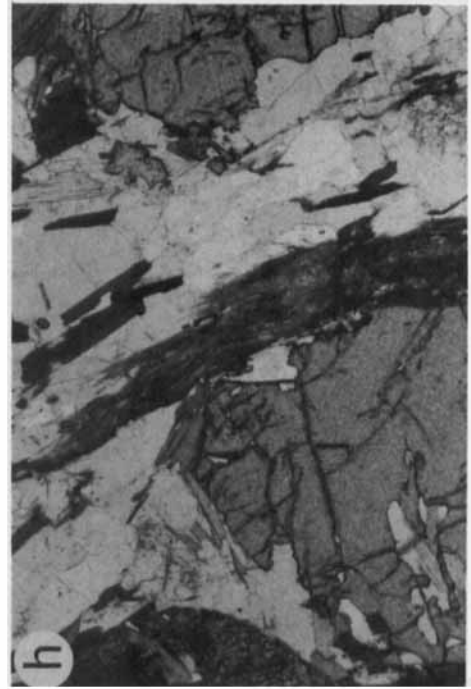
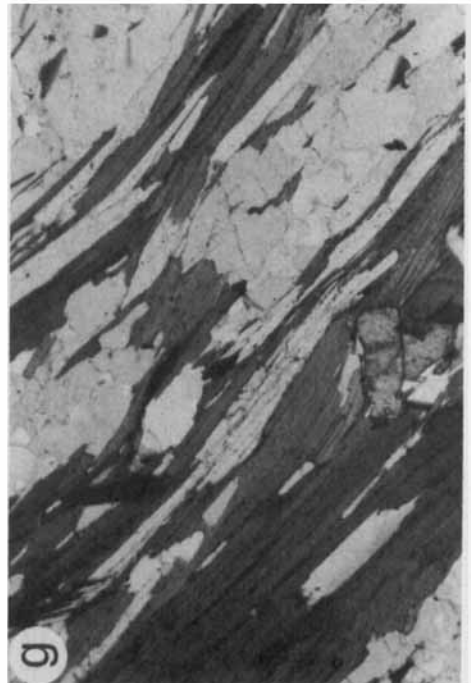
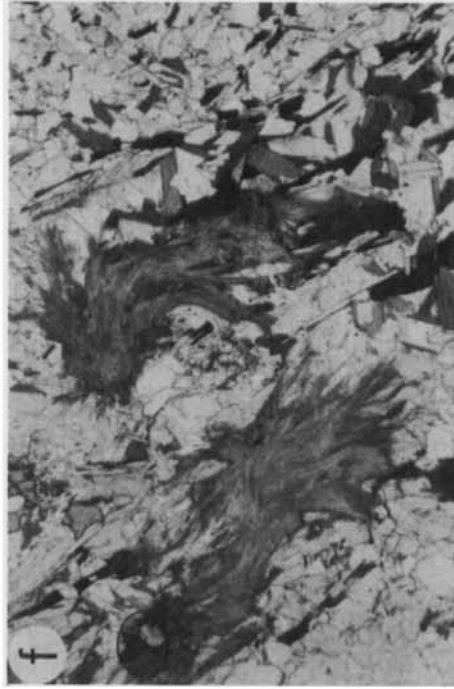


Figure 10. Photomicrographs of typical rock textures. Scale in all instances is the length of the long axis of photograph; all photographs taken in plane polarised light except for (d). (a)-(f) Shengus gneiss; (g)-(h) Iskere gneiss. (a) Crudely oriented sillimanite needles included in garnet (3.45 mm). (b) Ragged garnet rimmed by biotite-kyanite aggregate (3.45 mm). (c) Group of garnets (left) surrounded by biotite-kyanite aggregate. Thin bands in top right are also fine-grained biotite and kyanite; note how both minerals wrap, and are in contact with, orthoclase porphyroclast (6.63 mm). (d) Strained and recrystallized

orthoclase porphyroclast surrounded by quartz. Note recrystallized trails extending from grain edges and through grain centre (3-45 mm). (e) Ragged garnet surrounded by biotite-kyanite aggregate, which is streaked out parallel to quartz ribbons away from garnet. The lower aggregate, of similar appearance, is dominated by kyanite without garnet (6-63 mm). (f) Fibrolite mats and decussate muscovite aggregates (3-45 mm). (g) Shape fabric of muscovite and biotite, with small kyanite grain at bottom centre (3-45 mm). (h) Garnet and kyanite with later sillimanite mat (3-45 mm)



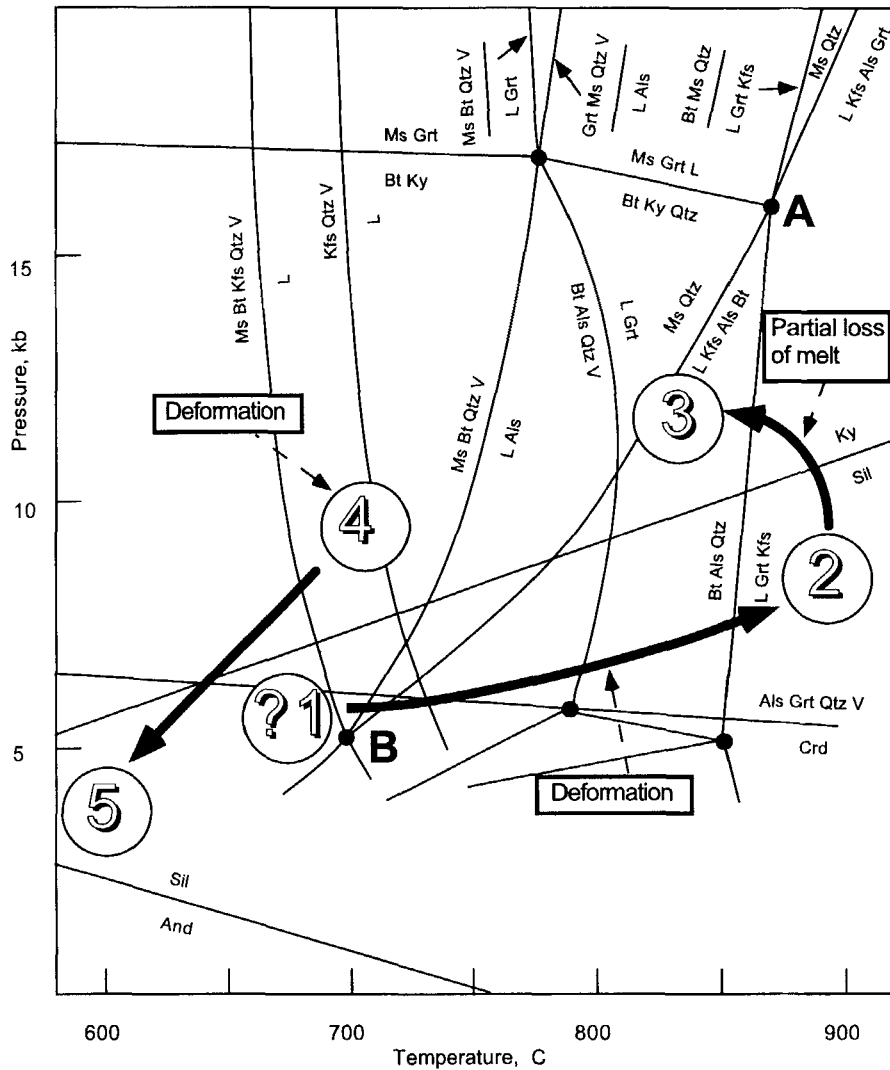
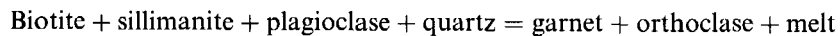


Figure 11. P-T grid showing important reactions in pelites at high temperatures, after Vielzeuf and Holloway (1988), and the approximate P-T 'path' deduced from mineralogy and textures in the Shengus gneisses. The univariant reaction lines which involve ferromagnesian phases are simplified representations of divariant fields, assuming a bulk rock Mg/(Mg+Fe) ratio of 0.5. In addition, some of the reaction lines were determined experimentally, not in a pure KFMASH system, but in a system containing albitic plagioclase, although its involvement is not indicated explicitly. The gap between stages 3 and 4 of the P-T path is to emphasize that these are parts of separate metamorphic cycles, separated in time by the episode of basic sheet emplacement. See text for details

is fairly likely as once any fluid-present melting line is crossed, the small amounts of fluid present in the rock would be consumed (e.g. Clemens and Vielzeuf 1987). If pressures were below those of invariant point A, an assemblage containing muscovite and biotite would first break down to an assemblage including orthoclase, aluminium silicate and melt; at higher temperatures, biotite would be involved in melting, with the production of garnet and more orthoclase. If pressures were above those of invariant point A, two melting reactions are again required, but on this path muscovite breakdown would be the higher temperature reaction. In either instance, we argue that stage 2 involved significant fluid-absent melting, including the breakdown of biotite. Although kyanite is present in the matrix, garnet overgrows sillimanite, so the full reaction would have been



We relate this partial melting episode, inferred from the assemblage, to the migmatitic banding seen in the field. Figure 11 shows that extreme temperatures of ca. 850°C are required; this estimate is not sensitive to pressure, as the reaction line is rather steep. However, it should be noted that Le Breton and Thompson (1988) found the onset of this reaction near 800°C at 10kbar, and that in detail it is sensitive to the Ti and F content of the biotite. We argued earlier that invariant point A must lie within the kyanite field: in this instance the temperature cannot be lower than that of the intersection of the ms+qtz breakdown curve and the ky = sil equilibrium, which is close to 800°C.

In stage 3, garnet reacted with a phase or phases that contained both H₂O and K₂O to form biotite and kyanite. This shows that the pressure had increased from that in stage 2, when sillimanite was the stable aluminium silicate polymorph. Two possible explanations for the reaction should be considered.

Firstly, garnet reacted with orthoclase, with H₂O being added from elsewhere. If H₂O were added as a fairly pure fluid phase, this could only occur at temperatures below all the solidi shown on Figure 11, otherwise further melting would ensue. Alternatively, H₂O moved by diffusion along grain boundaries, with $a_{\text{H}_2\text{O}} < 1$. Both instances require a water source. Pervasive re-introduction of H₂O into a large and dry migmatized region poses problems of fluid transport; it cannot be accomplished by diffusion on a large scale. Instead, the water could derive from crystallizing leucosome as the temperature decreased. This possibility was discussed by Waters (1988), although he presented evidence that in some granulites such water was lost rather than retained by reaction with restite.

Secondly, some rocks in which garnet is rimmed have no potassic phase other than biotite. This might be due to all the orthoclase being consumed in the above reaction, but alternatively it was the melt itself which reacted with garnet, supplying both H₂O and K₂O. If all the melt had been lost during migmatization, then back-reaction would not have been possible. The preservation of leucosomes on a centimetre scale shows that melt movement was not efficient. However, if all the melt had been retained, then complete back-reaction would have destroyed any mineralogical evidence for the melting: all the orthoclase would have been incorporated back into micas. Therefore, in this scenario we argue that *some* of the melt was segregated over distances across which it could not chemically interact with the restite. It would then be the dregs of melt, trapped in pores, which back-reacted. The first case, if the water is locally derived, has much in common with the second; in both, there must be a net water loss from the migmatites, otherwise the subsolidus assemblage would be completely regenerated. In the first case, water would be lost as a phase; this seems plausible as it has a low viscosity, however, at the temperature at which water would exsolve from the melt during cooling, it would be far from equilibrium with the restitic material through which it would have to percolate. So, notwithstanding Waters' (1988) interpretation of some migmatitic granulites, we consider this process problematic. In the second case, melt is postulated to be lost as a phase; this is also problematic, in view of its high viscosity, but the partial melt loss could have been aided if peak temperatures were yet higher than those that can be inferred from the final assemblage. High temperatures would increase the melt fraction and reduce its viscosity, both of which would aid melt loss. We prefer this hypothesis.

The biotite and kyanite are now intensely strained (e.g. Figure 10e) — the main LS shape fabric in these rocks was produced in stage 4. Thin section evidence cannot be used to distinguish whether this deformation is synchronous with the melt back-reaction. However, the basic sheets discussed earlier show no sign of being invaded by the leucosome from the migmatitic gneisses around them, although they are deformed along with the gneisses. We conclude that the basic sheets cut an essentially solid migmatite complex and that the main deformation post-dated both migmatite solidification and sheet intrusion — there remains the possibility that migmatization was Precambrian, whereas the later deformation was Himalayan. The relative timing is corroborated by the absence of any evidence for granulite facies metamorphism in the amphibolite sheets (see later). Stage 5 represents comparatively minor growth of new minerals, but shows that after the main deformation, in which kyanite was stable, conditions moved into the sillimanite stability field. It is only this stage, dominated by the recrystallization of earlier assemblages, which we assign to the Tertiary collision related metamorphism in this part of the Himalayas. The other stages are much earlier, as argued in the structural sections.

Electron microprobe data (available from the authors on request) were used in an attempt to constrain P–T conditions more tightly. Pressures and temperatures were calculated for nine high-grade Shengus

paragneisses which contain the basic low variance assemblage garnet–kyanite (+/– sillimanite)–plagioclase–orthoclase–biotite–quartz–rutile–+/– muscovite. Equilibria used to calculate metamorphic conditions were the garnet–biotite Fe–Mg exchange geothermometer of Ferry and Spear (1978) as modified by Hodges and Spear (1982) to account for non-ideality of mixing of minor components in garnet and by Indares and Martignole (1985) to account for Ti substitution in biotite; and the garnet–kyanite(sillimanite)–plagioclase–quartz geobarometer calibrated by Newton and Haselton (1981) and Koziol and Newton (1988). Analysed samples include a range from those with weak tectonic fabrics to those with ductile mylonitic fabrics characterized by annealed quartz ribbons and streaked out and aligned kyanite cleavage flakes. The major porphyroblastic phases (garnet and feldspars) show slight chemical compositional zonations: both plagioclase and orthoclase are slightly more albitic in rims than cores and garnet has slightly higher pyrope and spessartine contents and lower almandine contents in cores than rims. Minerals also showed chemical variations along rims.

Temperatures were calculated for each sample using a minimum of eight pairs of biotite rim–garnet rim compositions, and pressures for each sample by using a mean of a minimum of five garnet and plagioclase rim compositions. Despite the rigorous nature of the thermodynamic approach followed here, the calculated pressures and temperatures are, in many instances, inconsistent with the observed phase assemblages. For example, samples 33, 44 and 63, which are kyanite-bearing, plot in the sillimanite field. The calculated pressures and temperatures span a wide range of P–T space (Figure 12). Those samples which are the least deformed have the highest calculated pressures and temperatures, with the lower estimates coming from those samples with ductile mylonitic fabrics. This would be consistent with a re-equilibration of phase compositions during ductile deformation that post-dated the early migmatization. A number of textural and other criteria indicate that the calculated pressures and temperatures may not represent the P–T maxima. The common reaction rims of biotite and kyanite around garnet suggest that the biotite Fe/Mg ratio may not have been in equilibrium with that of garnet during growth. Ductile deformation involving recrystallization of kyanite and mafic phases, and the growth of late stage muscovite, are all suggestive of a complicated set of deformation and hydration events that post-date the metamorphic peak and which are likely to have upset the systematics of the exchange equilibria. A less well constrained, but likely, mechanism for further resetting the phase equilibria may be the thermal effects of leucogranite emplacement at shallow crustal levels during a late stage of post-metamorphic cooling and uplift. The highest pressure and temperature estimates (ca. 13 kbar and 840°C) derived from sample SG are consistent with observed mineral assemblage data in that they fall within the kyanite field and at temperatures above that of the vapour-absent melting of muscovite. It is interesting to note that temperature estimates scatter down to near the effective 'closure' temperature for Fe–Mg diffusion in garnet (Yardley 1977), which would be compatible with partial diffusive re-equilibration. Nevertheless, in view of the scatter in these P–T estimates, we prefer to infer pressures and temperatures on the basis of phase petrology constraints. Figure 11 shows the approximate P–T path deduced.

4c. Iskere gneiss: textures

In contrast with the Shengus gneiss, the Iskere gneisses in the samples we have studied contain either orthoclase or aluminium silicate but never both, and muscovite is often foliated parallel to biotite (Figure 10g). Moreover, orthoclase never occurs together with garnet. The aluminium silicate phase is normally fibrolite, as mats within the foliation (Figure 10h), but occasionally kyanite porphyroblasts are also present. There are no well-developed reaction textures between any of these phases.

4d. Iskere gneiss: interpretation

Referring to Figure 11, the dominant foliation appears to have formed within the stability field of muscovite and biotite. The key mineral pairs of orthoclase — aluminium silicate and orthoclase — garnet which, it was argued earlier, indicate partial melting, are absent. However, in the field the rocks are migmatitic, with leucosomes bordered by biotite selvages in places. It is possible that this banding was

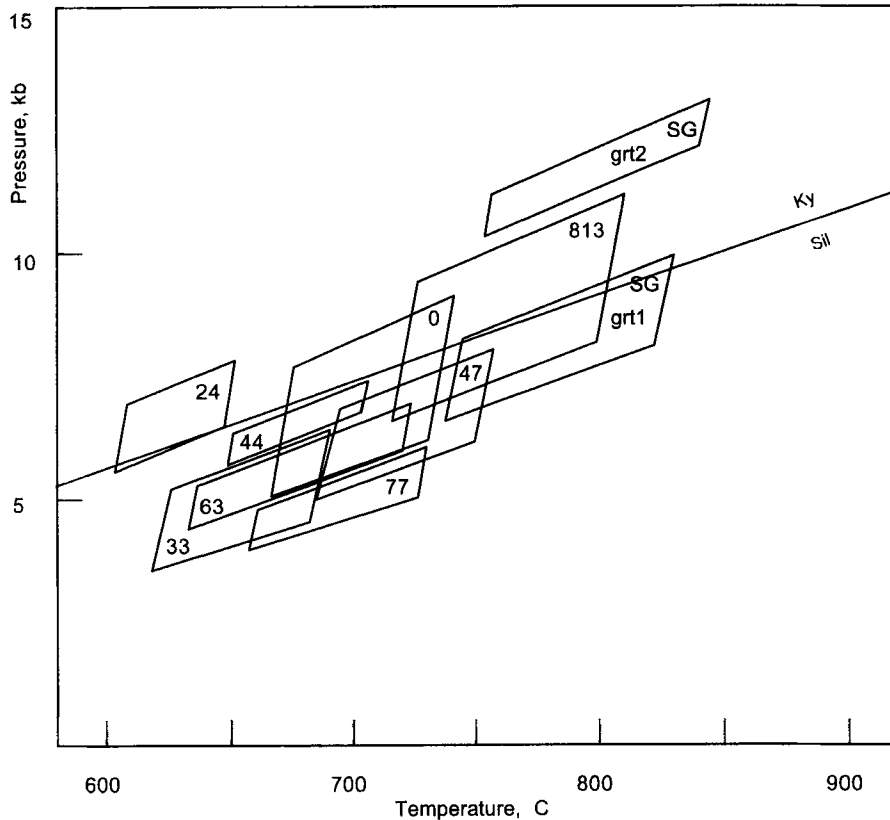


Figure 12. P-T estimates deduced for different samples of Shengus gneiss from geothermobarometry. For each sample, the sides of the P-T 'fields' represent the maximum and minimum pressures and temperatures deduced from different rim compositions

formed by subsolidus processes, or by melt injection, or by eutectic fluid-present melting of orthoclase-plagioclase-quartz at temperatures within the muscovite stability field. In each instance, the P-T history of the Iskere gneisses would be different to that of the Shengus gneisses; but, within the Shengus paragneisses, some grey gneisses show foliated muscovite and biotite and look similar to the Iskere grey gneisses (e.g. NP67), yet are likely to have shared the Shengus gneiss history. We propose a model in which both units experienced the same P-T history, although there is a possibility that later tectonism interleaved rocks with different histories.

In the Iskere gneisses, if they experienced granulite facies conditions, it is inevitable that partial melting was extensive and related to dehydration of micas in the absence of fluid. Then, in contrast with the Shengus gneiss, we suggest melt was almost entirely retained. This would allow the back-reaction of melt with restite to go to completion, even though modal banding associated with small-scale melt segregation is preserved. Muscovite and biotite would form by peritectic reactions between garnet, aluminium silicate and orthoclase and melt. The preservation of felsic bands marking the position of melt segregations could relate to the detailed processes of back-reaction. For instance, during back-reaction biotite may have formed by growth of residual biotite in the melanosome (with diffusion of appropriate elements through the melt), rather than by nucleating new biotite in the leucosome. Alternatively, the melt crystallized, without interacting chemically with the melanosome, until water was released which could then move and react with the melanosome. These and other processes would allow the preservation of partial melt textures on the centimetre scale even if the melt has back-reacted. As argued for the Shengus gneiss, the main deformation was much later than the back-reaction. Any grain-scale textural evidence for back-reaction could have been erased by this later strain. This is our preferred explanation for the Iskere gneiss migmatization.

Kyanite is found in a few thin sections, slightly wrapped by the muscovite–biotite foliation, and was the stable polymorph during deformation, with sillimanite mats developing later. In this scheme, the P–T history of the Iskere gneisses need not have been very different from that of the Shengus gneiss, although their bulk-rock chemistries differ. The preserved part of the history of the Iskere gneisses is compatible with stages 4 and 5 (Figure 11) and it is possible that they experienced the same peak conditions as the Shengus gneiss.

In our interpretation one of the key differences in the histories of the two gneiss groups is the extent to which melt was lost during migmatization, rather than the difference in P–T paths. We speculate that this is due to the amount of melt produced: large melt fractions can be lost more easily than small melt fractions. A key melting reaction was that involving kyanite, biotite and plagioclase. Such melting would be limited by the amount of kyanite present; metapelites, being aluminous, might be expected to have more of this phase than granitoids, and thus could produce more melt. If the relatively large metapelite melt fraction was partly lost, whereas that in the metagranitoids was retained, then the observed contrasts in the two gneiss groups would result.

4e. *Metamorphism of the basic sheets*

The basic sheets carry hornblende and plagioclase with or without garnet, biotite, epidote, sphene and accessory minerals. The dominant fine-grained plagioclase and hornblende form aggregates defining an LS shape fabric. Two thin sections show, in addition, pyroxene rimmed by very fine-grained amphibole and, in one of these, plagioclase is also present intergrown with the pyroxene in an ophitic texture. We infer that the amphibolite facies metamorphism and deformation directly overprinted the original igneous mineralogy and textures. Importantly, there is no evidence that the basic sheets were in granulite facies either during metamorphism (no syntectonic pyroxene) or at any stage before it (relict pyroxenes retain igneous, not metamorphic, textures). The amphibolite facies assemblage does not tightly constrain the pressure or temperature, but is compatible with the grade of the main deformation, in which biotite and kyanite were stable in the gneisses surrounding the basic sheets. There is no evidence that the basic sheets began to dehydrate to form pyroxene-bearing assemblages, which might be expected at temperatures $> 800^{\circ}\text{C}$ experienced by the pelites during migmatization. This is compatible with the hypothesis that the dykes were injected after migmatization.

4f. *Summary of metamorphic data*

The Indus gorge gneisses have experienced both high pressures and high temperatures, as epitomised by partial melting of metapelites with the production of garnet and orthoclase. This pre-dated the intrusion of basic sheets and was therefore pre-Himalayan, unless the sheets were intruded at some time during the Himalayan orogeny. The post-basic sheet P–T ‘path’ we give in Figure 11 was synchronous with deformation dated as Himalayan on structural grounds and resembles the history deduced by Pognante *et al.* (1993) for gneisses within the syntaxis further north.

5. DISCUSSION

The Nanga Parbat syntaxis evolved as follows. Metapelites and metagranitoids, partly of Precambrian origin, were deformed and migmatized in the granulite facies at temperatures high enough to cause dehydration melting of biotite. Melt was lost from some migmatites, but retained in others. Though the Iskere and Shengus gneisses might have had similar metamorphic histories, these could have been widely separated in time and other events may have affected them. The solidified migmatite complex was intruded by a suite of basic sheets. All of this history is likely to pre-date the Tertiary Himalayan collision, unless the possibility of post-collision basic magmatism is admitted. The earliest collision-related structures seen are the pervasive foliation and lineation seen in both gneisses and basic sheets, and formed in the amphibolite facies. This deformation caused intense recrystallization of much earlier amphibolite facies assemblages,

which were formed on the retrograde path of the early metamorphism. There are no obvious grade differences across the syntaxis: kyanite was the stable aluminium silicate during deformation, with sillimanite locally developed later after deformation ceased. The deformation was associated with the overthrusting of the Kohistan–Ladakh island arc material, also recording amphibolite facies, and local interleaving of this with the Indian plate gneisses. Later, this thick zone of amphibolites began to shorten perpendicular to the transport direction. Such lateral shortening was a result of differing movement directions of the Ladakh and Kohistan parts of the Himalayan thrust belt, as recorded in the regional lineation pattern (Brunel 1985); the cause may relate to pinning of the main Himalayan thrusts (Coward *et al.* 1986; Treloar *et al.* 1991). Shortening produced a large, tight antiformal structure which affected fabrics subparallel to the MMT and in its footwall. At some time after this fold formed, garnet granite sheets and pegmatites were injected. These may have been formed from the anatexis of crustal rocks, but as we have no evidence for partial melting of this age in the Indus gorge transect, the source region may still be deeply buried. The latest stages of syntaxis evolution are currently the subject of geochronological study and will be detailed elsewhere.

The Indus gorge gneisses are very different from those studied by Zeitler *et al.* (1993) in the Tato area to the south; these differences may be due to different pressure–temperature–time histories, but variations in bulk-rock compositions could also be pertinent, which might have an effect on whether rock units register particular metamorphic reactions. In the Tato area, migmatites carry cordierite, without kyanite, and so preserve a lower pressure (and probably much younger) melting history than those of the Indus gorge. To the north of the Indus gorge, in the Stak valley, kyanite migmatites were described by Pognante *et al.* (1993), who infer an exhumation path involving cooling during pressure decrease. Amphibolites in that area carry clinopyroxene, so there may be differences in P–T histories between the Indus and Stak valleys. There may also be differences in protolith; Butler *et al.* (1992) showed that, east of Haramosh, an important group of rocks (the ‘Layered Unit’) is found, different to both the Shengus and Iskere gneisses, and this may continue to the Stak valley.

Existing geochronological work has yielded young ages from the Iskere gorge, some of which are crystallization, not cooling, ages. Smith *et al.* (1992) document U/Pb ages of ca. 9 Ma for the rims of monazites from the Iskere gneisses. Such age data do not conflict with our interpretation of an earlier migmatization event as monazite can grow at amphibolite facies (Smith and Barreiro 1990): partial melting is not a prerequisite, even if elsewhere in the massif monazite is interpreted to have grown during very recent migmatization (Zeitler *et al.* 1993). This highlights the need to refer to *specific* metamorphic events in regard to dating polymetamorphic regions. A date from, for instance, a monazite rim can only be tied to other petrographic features if the details of the monazite-forming reaction are understood. It could be a prograde, peak or retrograde reaction. More work is needed to clarify the timing of the various metamorphic events both here and elsewhere in the Nanga Parbat syntaxis; field, petrographic and geochronological techniques are all integral to this task.

6. CONCLUSIONS

1. Field relationships, in particular the suite of basic sheets cross-cutting earlier metamorphic features, are the key to understanding this polymetamorphic terrane. Earlier, pre-Himalayan metamorphism was at granulite facies and involved migmatization; later, Himalayan metamorphism was at amphibolite facies.
2. During the granulite facies migmatization, melt mobility in different gneiss types played an important part in determining their final mineralogy and texture. The physical and chemical behaviour of melt, and its possible back-reaction with restite assemblages, should be taken into account when studying such granulite terranes.
3. Mineral growth ages in this and other polymetamorphic terranes carry limited information unless that mineral growth or recrystallization is tied to a *particular* metamorphic episode via a textural interpretation.
4. Himalayan foliations were folded into a tight antiform without the production of new fabrics, although shearing on the western margin produced new fabrics during relative uplift of the syntaxis.

5. Granites thought to be derived by partial melting of crust are not necessarily genetically related to migmatite complexes which they intrude. In the Indus gorge, anatexis was followed by solidification, the intrusion of basic sheets and deformation before the emplacement of granite sheets. The migmatization event did not give rise to the younger granite sheets.

ACKNOWLEDGEMENTS

We thank R. Butler and D. Prior for useful comments, and N. Charnley of Oxford University for assistance with electron microprobe analysis. This work was funded by NERC research grant GR3/6113 (to M. Coward) on Himalayan tectonics. J.W. acknowledges NERC postdoctoral fellowship GT5/F/88/GS/1.

REFERENCES

- Bossart, P., Dietrich, D., Greco, A., Ottiger, R. and Ramsay, J. G. 1988. The tectonic structure of the Hazara–Kashmir syntaxis, Southern Himalayas, Pakistan. *Tectonics* **7**, 273–297.
- Brunel, M. 1985. Ductile thrusting in the Himalayas: shear sense criteria and stretching lineations. *Tectonics* **5**, 247–265.
- Butler, R. W. H. and Prior, D. J. 1988a. Anatomy of a continental subduction zone: the Main Mantle Thrust in Northern Pakistan. *Geologisches Rundschau* **77**, 239–255.
- — — and — — — 1988b. Tectonic controls on the uplift of the Nanga Parbat massif, Pakistan Himalayas. *Nature* **333**, 247–250.
- — —, — — — and Knipe, R. J. 1989. Neotectonics of the Nanga Parbat syntaxis, Pakistan, and crustal stacking in the northwest Himalayas. *Earth and Planetary Science Letters* **94**, 329–343.
- — —, George, M., Harris, N. B. W., Jones, C., Prior, D. J., Treloar, P. J. and Wheeler, J. 1992. Geology of the northern part of the Nanga Parbat massif, northern Pakistan, and its implications for Himalayan tectonics. *Journal of the Geological Society, London* **149**, 557–567.
- Chamberlain, C. P., Zeitler, P. K. and Jan, M. Q. 1989. The dynamics of the suture between the Kohistan island arc and the Indian plate in the Himalaya of Pakistan. *Journal of Metamorphic Geology* **7**, 135–149.
- Clemens, J. D. and Vielzeuf, D. 1987. Constraints on melting and magma production in the crust. *Earth and Planetary Science Letters* **86**, 287–306.
- Coward, M. P. 1985. A section through the Nanga Parbat syntaxis, Indus valley, Kohistan. *Geological Bulletin of the University of Peshawar* **18**, 147–152.
- — —, Windley, B. F., Broughton, R. D., Luff, I. W., Petterson, M. G., Pudsey, C. J., Rex, D. C. and Asif Khan, M. 1986. Collision tectonics in the NW Himalayas. In: Coward, M. P. and Ries, A. C. (eds) *Collision Tectonics*. Geological Society, London, *Special Publications* **19**, 203–219.
- Ferry, J. M. and Spear, F. S. 1978. Experimental calibration of the partitioning of Fe and Mg between biotite and garnet. *Contributions to Mineralogy and Petrology* **66**, 113–117.
- Hodges, K. V. and Spear, F. S. 1982. Geothermometry, geobarometry and the Al_2SiO_5 triple point at Mt. Moosilauke, New Hampshire. *American Mineralogist* **67**, 1118–1134.
- Indares, A. and Martignole, J. 1985. Biotite–garnet geothermometry in the granulite facies: the influence of Ti and Al in biotite. *American Mineralogist* **70**, 272–278.
- Kozlowski, A. M. and Newton, R. C. 1988. Redetermination of the garnet breakdown reaction and improvement of the plagioclase–garnet– Al_2SiO_5 –quartz geobarometer. *American Mineralogist* **73**, 216–223.
- Kretz, R. 1983. Symbols for rock-forming minerals. *American Mineralogist* **68**, 277–279.
- Le Breton, N. and Thompson, A. B. 1988. Fluid-absent (dehydration) melting of biotite in metapelites in the early stages of crustal anatexis. *Contributions to Mineralogy and Petrology* **99**, 226–237.
- Madin, I. P., Lawrence, R. D. and Ur-Rehman, S. 1989. The northwestern Nanga Parbat–Haramosh massif; evidence for crustal uplift of the northwestern corner of the Indian craton. In: Malinconico, L. L. and Lillie, R. J. (eds) *Tectonics of the Western Himalayas*. Geological Society of America, *Special Publications* **232**, 169–182.
- Misch, P. 1949. Metasomatic granitization of batholithic dimensions. *American Journal of Science* **247**, 209–245.
- Newton, R. C. and Haselton, M. T. 1981. Thermodynamics of the garnet–plagioclase– Al_2SiO_5 –quartz geobarometer. In: Navrotsky, A. and Wood, B. J. (eds) *Thermodynamics of Minerals and Melts*, Springer-Verlag, New York, 131–147.
- Pognante, U., Benna, P. and Le Fort, P. 1993. High-pressure metamorphism in the High Himalayan Crystallines of the Stak valley, north-eastern Nanga Parbat–Haramosh syntaxis, Pakistan Himalaya. In: Treloar, P. J. and Searle, M. P. (eds) *Himalayan Tectonics*. Geological Society, London, *Special Publications* **74**, 161–172.
- Pudsey, C. J. 1986. The Northern Suture, Pakistan: margin of a Cretaceous island arc. *Geological Magazine* **123**, 405–423.
- Smith, H. A. and Barreiro, B. 1990. Monazite U–Pb dating of staurolite grade metamorphism in pelitic schists. *Contributions to Mineralogy and Petrology* **105**, 602–615.
- — —, Chamberlain, C. P. and Zeitler, P. K. 1992. Documentation of Neogene regional metamorphism in the Himalayas of Pakistan using U–Pb in monazite. *Earth and Planetary Science Letters* **113**, 93–105.
- Sutton, J. and Watson, J. V. 1951. The pre-Torridonian metamorphic history of the Loch Torridon and Scourie areas in the NW Highlands and its bearing on the chronological classification of the Lewisian. *Journal of the Geological Society, London* **106**, 241–308.
- Tonarini, S., Villa, I. M., Oberli, F., Meier, M., Spencer, D. A., Pognante, U. and Ramsay, J. G. 1993. Eocene age of eclogite metamorphism in Pakistan Himalaya: implications for India–Eurasia collision. *Terra Nova* **5**, 13–20.

- Treloar, P. J., Broughton, R. D., Williams, M. P., Coward, M. P. and Windley, B. F. 1989a. Deformation, metamorphism and imbrication of the Indian plate, south of the Main Mantle Thrust, north Pakistan. *Journal of Metamorphic Geology* **7**, 111–125.
- — —, Rex, D. C., Guise, P. G., Coward, M. P., Searle, M. P., Windley, B. F., Petterson, M. G., Jan, M. Q. and Luff, I. W. 1989b. K–Ar and Ar–Ar geochronology of the Himalayan collision in NW Pakistan: constraints on the time of suturing, deformation, metamorphism and uplift. *Tectonics* **8**, 881–909.
- — —, Potts, G. J., Wheeler, J. and Rex, D. C. 1991. Structural evolution and asymmetric uplift of the Nanga Parbat syntaxis, Pakistan Himalaya. *Geologisches Rundschau* **80**, 411–428.
- Vannay, J. C. and Spring, L. 1993. Geochemistry of the continental basalts within the Tethyan Himalaya of Lahul-Spiti and SE Zaskar, northwest India. In: Treloar, P. J. and Searle, M. P. (eds) *Himalayan Tectonics*. Geological Society, London, *Special Publications* **74**, 237–249.
- Vielzeuf, D. and Holloway, J. R. 1988. Experimental determination of the fluid-absent melting relations in the pelitic system. *Contributions to Mineralogy and Petrology* **98**, 257–276.
- Wadia, D. N. 1931. The syntaxis of the north-west Himalaya, tectonics and orogeny. *Records of the Geological Survey of India* **65**, 189–220.
- — — 1932. Note on the geology of Nanga Parbat (Mt. Diamir), and adjoining portions of Chilas, Gilgit district, Kashmir. *Records of the Geological Survey of India* **66**, 212–234.
- Waters, D. J. 1988. Partial melting and the formation of granulite facies assemblages in Namaqualand, South Africa. *Journal of Metamorphic Geology* **6**, 387–404.
- Yardley, B. W. D. 1977. An empirical study of diffusion in garnet. *American Mineralogist* **62**, 793–800.
- Zeitler, P. K. 1985. Cooling history of the NW Himalaya, Pakistan. *Tectonics* **4**, 127–131.
- — —, Sutter, J. F., Williams, I. S., Zartman, R. and Tahirkheli, R. A. K. 1989. Geochronology and temperature history of the Nanga Parbat–Haramosh Massif, Pakistan. In: Malinconico, L. L. and Lillie, R. J. (eds) *Tectonics of the Western Himalayas*. *Geol. Soc. Am. Spec. Pub. No. 232*, 1–22.
- — —, Chamberlain, C. P. and Smith, H. A. 1993. Synchronous anatexis, metamorphism and rapid denudation at Nanga Parbat (Pakistan Himalaya). *Geology* **21**, 347–350.